16th World Conference on Earthquake Engineering, 16WCEE 2017
Santiago Chile, January 9th to 13th 2017
Paper N° 1004 (Abstract ID)
Registration Code: S-C1464728773

PERMANENT DISPLACEMENT FROM SURFACE-RUPTURING EARTHQUAKES: INSIGHTS FROM DYNAMIC RUPTURE OF Mw7.6 1999 CHI-CHI EARTHQUAKE

L.A. Dalguer(1), K. Irikura(2), H. Wu(3)

(1) *Structural Engineer and Seismologist, Swissnuclear, Switzerland, luis.dalguer@swissnuclear.ch*
(2) *Professor, Aichi Institute of Technology, Japan, kojiroirikura@gmail.com*
(3) *Post-doctoral researcher, Aichi Institute of Technology, Japan, haowuseis@gmail.com*

Abstract

Large permanent displacements, sometimes named "fling", resulted from surface-rupturing faulting have been observed in some earthquakes, such as the 1999 Kocaeli, 1999 Chi-Chi, 2002 Denali, reaching amplitudes over 8 m. This type of near-source ground motion is different from ordinary ground motion often evaluated by engineers and seismologist, for example to derive traditional ground motion prediction equations or to conduct seismic hazard studies. These permanent displacements are formed from coherent long period velocity pulses caused mainly by the offset of the ground surface when fault-rupture extends to the earth surface. To further investigate this type of ground motion, we developed dynamic rupture simulations of the Mw7.6 1999 Chi-Chi, Taiwan earthquake using asperity models in which the shallow layer (SL) of the first 2km depth is assumed to operate during rupture with enhanced energy absorption mechanism, as such it is parameterized with negative stress drop. Our physics-based dynamic rupture models show that the velocity ground motion causing permanent displacement near the source is dominated by the energy carried by the slip velocity pulse at the shallow layer fault of the first 2km depth, though this shallow zone is characterized with negative or zero stress drop. The asperities are the main driver elements to break the shallow layer and free-surface, but if surface rupture is not allowed, the rupture is inhibited to extend along strike, consequently the velocity pulse causing permanent displacement is reduced significantly. This study suggests that the slip velocities at the shallow fault zone, in which zero or negative stress drop operates, are the main source causing strong velocity pulses causing permanent displacement near the source. Therefore, when using simplified models, such as kinematic models, to study near source ground motion of surface-rupturing earthquakes, these slip velocity functions at the shallow zone have to be carefully considered.

Keywords: Permanent displacement, surface rupture, dynamic rupture simulation, slip velocity function, near-source ground motion.

1. Introduction

Permanent ground displacement, named also as “fling” in the earthquake engineering community [e.g., 1, 2, 3], is usually observed from large earthquakes, especially in surface-rupturing events, in which this offset can be significantly large near the fault reaching amplitudes over 1.0 to 10 m, as has been observed in some events such the 1999 Kocaeli [e.g. 4], 1999 Chi-Chi [e.g. 5, 6], 2002 Denali [e.g. 7], 2008 Wenchuan [e.g. 8], 2011 Tohoku [e.g. 9]. These permanent displacements are dynamically formed from coherent long period velocity pulses (known as “fling-pulse”) in the direction of the fault slip and it is significantly amplified by the offset of the ground surface when fault-rupture extends to the earth surface. These fling-pulses are different from those caused by forward directivity [e.g. 10], in which the velocity pulse is enhanced in the direction normal to the fault slip and does not produce amplified permanent displacement. Though the fling-pulse and the corresponding permanent displacement is understood in general to be an effect of the permanent tectonic deformation caused by a rupturing fault, little attention has been down to evaluate the source where waves are radiating to produce such pulses, that is, the slip velocity function causing fling-pulses. In this paper we focus on the shallow zone of the rupturing-fault. For that purpose, we develop a dynamic rupture simulation of the Mw7.6 1999 Chi-Chi Taiwan earthquake. The fault is characterized with simple asperities models to define the fault rupture to investigate the slip velocity function at the shallow layer (SL). The SL of the first 2km depth is assumed to operate during rupture with enhanced energy absorption mechanism, as such it is parameterized with negative stress drop [e.g. 11, 12]. We show that this SL fault zone, even in such conditions defined here, are the main source causing strong velocity pulses causing strong ground motion and permanent displacement near the source. Suggesting that these slip velocity functions at the SL have to be carefully considered when developing models for ground motion prediction.

2. General methodology for asperity model parameterization

The fault is represented by asperity areas named as Strong Motion Generation Areas (SMGA), as defined by Miyake et al [13] and Irikura and Miyake [14], and background areas. The asperities are characterized with high stress drop compared to the background. Within this concept, the methodology and procedure to parameterize this type of fault models are as follow:

1) Define rupture area: if there is not a target event in which rupture area is known, it can be derived from an empirical scaling relations [e.g.14,15,16, 17, 18, 19]
2) Define asperity area. In this study we use the characteristic slip models proposed by Somerville et al. [16]. These authors analyzed kinematic images from source inversions of past earthquakes and proposed two main statistical properties: i) the average of combined asperity area is 0.22 times the total rupture area; ii) average slip on the combined asperities is 2 times the average slip over all the fault.
3) Define stress drop ratio between average stress drop on asperities and background stress drop. Dalguer et al. [11, 20] estimated these rations calibrating asperity dynamic rupture models constrained with the kinematic characterization of Somerville et al. [16]. The general tendency is that stress-drop ratios are in the range of 0.05 to 0.1 for buried earthquakes and -0.15 to 0.05 for surface-rupturing
4) Define average dynamic stress drop: Dalguer et al. [11, 20] calibrated dynamic asperity models that fit the empirical scaling relations. This calibration permits estimating the average stress drops consistent with the empirical scaling model. From these calibration, these authors proposed a variation of average stress drop depending on the ratio L/W, where L and W are respectively the length and width of the fault.
5) Define absolute values of stress drop on asperity areas. If available a kinematic source slip distribution, the stress drop distribution from the kinematic model can be estimated solving the elastodynamic equations [e.g. 21,22] and then define asperity areas following Somerville et al. [16]. Another procedure is following the method of Kamae and Irikura [23] in which the parameters seismic moment and stress drop are quantified by forward modeling using the empirical Green's function method while assuming the asperities at segments with large slips in the fault plane based on the results of waveform inversion. They applied this model to the 1995 Hyogoken-Nambu Earthquake.

6) The steps described until 5 serve to define initial values of the stress drop distribution. These values may need refinement by trial and errors to fit the target event, such as slip distribution and moment magnitude.

3. Parameterization of the Shallow Layer (SL)

It is well accepted by the community that the rupture at the SL may operates in a distinctive manner from the rest of the fault. This is due to the formation of incompetent fault gouge, cracking [e.g. 24, 25], presence of thick surface deposits of sediments, fissured rocks and other forms of brittle rock damage that have evolved over many earthquake cycles and may even have formed flower-like zone structures with significant shallow damage that decreases in amplitude and width with depth [e.g. 26, 27, 28, 29, 30]. These shallow weak zones are maybe formed because the normal stress is depth dependent. Therefore, the shallow strength is limited to the weight of the overburden (as in normal faulting environments) that is not able to maintain large shear stresses [e.g., 23] and therefore can easily damage or fracture. This damage zone can be accumulated during the lifetime of a fault, either as the result of dynamic stress change induced by rupture during an earthquake [e.g., 26, 27, 28, 29] or from quasi static deformation during the life of a shear fault [e.g., 31]. The main feature of this shallow depth zone is that it operates during rupture with an enhanced energy absorption mechanism. This makes the frictional properties of the shallow zone be distinct from those at deeper levels [e.g. 32, 33]. This zone can be characterized by velocity strengthening friction. To approximately mimic this mechanism, we impose a negative stress drop at shallow depth. And to account for the fault strength depth dependent in this shallow zone, the relative strength of the fault is reduced when approaching to the free-surface. For the case study in this paper, we define the first 2 km depth as the weak shallow zone. It is worthy to notice that if this shallow depth is not parameterized in an appropriate way, early and unphysical rupture process may take place in this zone.

4. Asperity model for the 1999 Chi-Chi, Taiwan, Earthquake

The Chi-Chi, Taiwan, earthquake (Mw 7.6) of 20 September 1999 originated on a low angle reverse fault with a strike of nearly N5ºE and a dip between 25º and 36º [34]. The rupture of the causative fault reached the surface and propagated along about 80 km, starting in the south and extending northward on the Chelongpu fault. Spectacular horizontal displacements up to 9.0 m and vertical offsets of 1.0 to 8.0 m were registered along the surface rupture.

The parameterization of the asperity model follows the methodology procedure described above and is guided by the slip [35] and stress drop [36] distribution derived from the results of source inversion [35]. We also used as guideline the asperity model proposed by Ikeda et al [37]. We assume a fault rupture area of 79km length and 39km width with dip angle of 29º. We use the simple slip weakening friction model in the form given by Andrews [38]. The dynamic rupture and near-source ground motion simulations are developed using the Support Operator Rupture Dynamics code (SORD) from Ely et al., [39]. After trial and error we propose an asperity model with five asperities as shown in Fig. 1 for dynamic rupture simulation that approximately fits the target event in term of slip distribution, rupture duration and moment Magnitude. Fig. 1 shows the stress drop, strength excess and critical slip distance (Dc) distribution. Dc is assumed to be larger at the northern asperities than those at the southern. The largest Dc is at the shallow weak zone with 2km depth. Strength excess at the shallow zone decrease when approaching the free-surface, stress drop is negative in this zone with the largest values at the northern. The back ground stress drop in the rest of the fault is assumed to be zero. Fig 2 shows the asperity fault model placed on the geographic map with the trace of the Chelongpu fault.

The different parameterization between southern and northern was set in order to be consistent with the observed feature that characterized this earthquake. As described by Dalguer et al [40], this earthquake ruptured the southern and northern in a different manner, as reflected in the structural damage pattern distribution. Although the strongest ground motion occurred near the northern part of the trace, structural damage was heavier in the southern part. The difference seems to be in the frequency content of ground motion radiation from the source. Southern radiated higher ground motion capable to damage building, while the northern was stronger at low frequency. In order to reproduce this feature, frictional parameters need to be different in the northern and southern. The northern needs to be characterized by large fracture energy (consequently large Dc) and the shallow zone at the northern with larger energy absorption mechanism than the southern part.

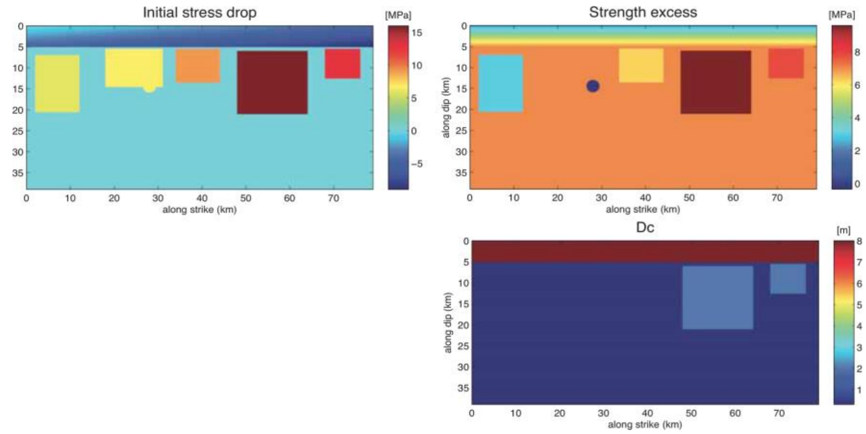

Fig. 1 Proposed asperity source model for this study for dynamic rupture simulation. Left shows stress drop distribution, top right strength excess and bottom right critical slip distance (Dc).

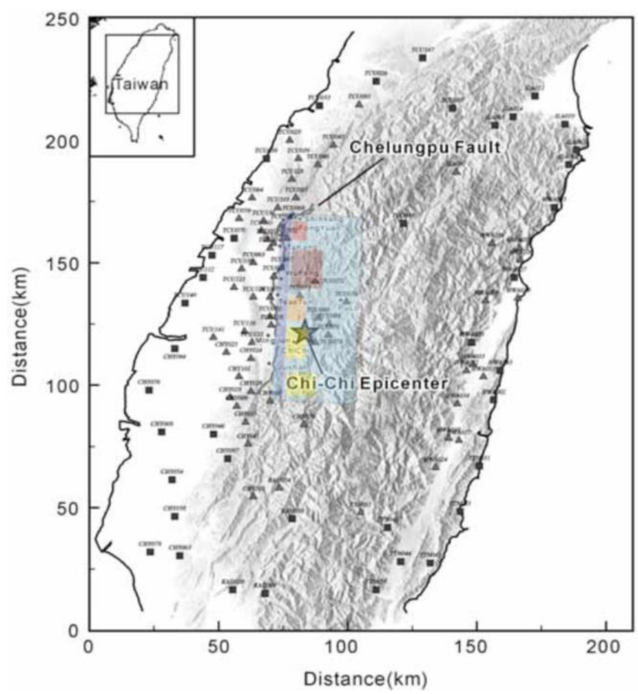

Fig. 2 Location of the proposed asperity source model on the geographic map with the trace of the Chelongpu fault and epicenter of the 1999 Chi-Chi, Taiwan, earthquake.

5. Simulation results

5.1 Source rupture solution

Figure 3 shows the dynamic rupture solution represented by the final slip, peak slip velocity, rupture speed and rupture time distribution along the fault. The simulation produces a moment magnitude of Mw=7.64. Slip distribution is consistent with the slip distribution obtained from source inversion with the large slip at the northern asperity. Rupture breaks about 75% of the free-surface that interacts with the ruptured fault, with the largest offset of about 10m at the northern side, that is consistent with the observations. Peak slip velocity (obtained directly from the simulation without filtering) is also dominated by the asperities, suggesting that most of the seismic radiation energy come from the asperities. Notice that at the shallow zone large slip velocities is observed, specially at the northern site. A close looks of the slip velocity function at different points on the fault is shown in Figure 4. These slip velocity waveforms are low pass filtered with a frequency cut of 3.0Hz (the maximum frequency resolvable in our simulation is 2.0Hz). Even though the shallow zone is dominated by negative stress drop, seismic radiation is maybe considerable from this zone due to the large slip velocity. Rupture speed accelerates at the asperities and slow down when enter into the background. This is clearly observed at contour plot that overlap the slip and peak slip distribution. The rupture speed at the shallow zone is very complex with acceleration and deaccelerations processes. The free-surface play an important role to accelerate the rupture. The rupture reaches the northern part after about 26 seconds.

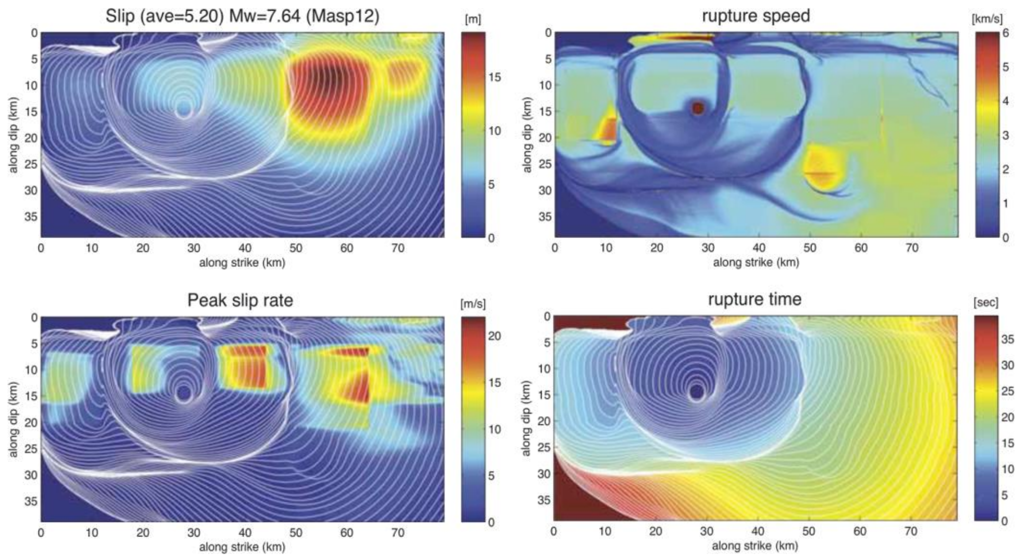

Fig. 3 Dynamic rupture solution represented by the final slip distribution (top left), peak slip velocity (bottom left), rupture speed (top right) and rupture time (bottom right). Contour lines on the slip and peak slip rate images are the rupture time each 0.5 seconds

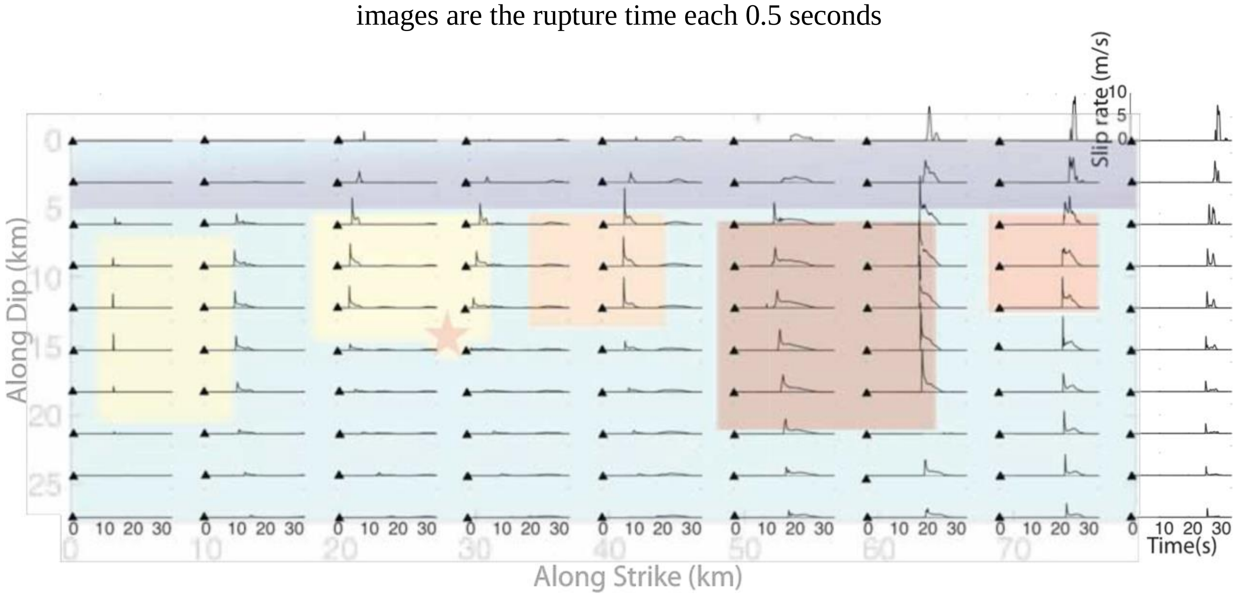

Fig.4. Slip velocity functions resulted from the dynamic rupture simulation at selected points on the fault. These slip velocity waveforms are low pass filtered with a frequency cut of 3.0Hz.

5.2 Fault displacement and ground motion compared with observed data

Figure 5 shows the fault displacement of our preferred model compared with the observed data. Overall the fault displacement along the fault is consistent with the observed data. These results can be improved by tuning the weak shallow zone.

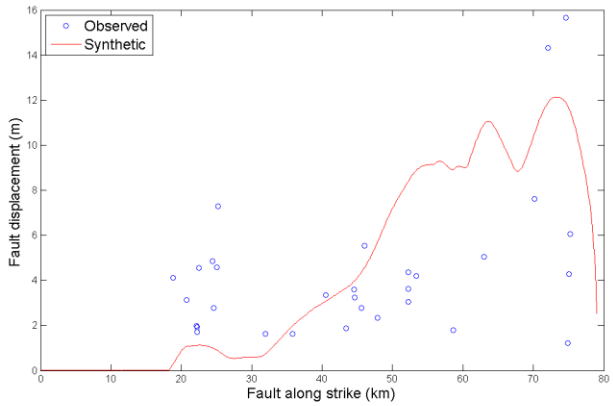

Fig. 5. Fault displacement compared with observed data [41]

The 3 components of velocity and displacement compared with observed data [42] at some stations with permanent displacement are shown in Fig. 6. Seismograms passed a low pass filter with frequency cut off of 0.5Hz. In all the figures, left column are velocity and right column displacement of three components (EW, NS and UD). In general synthetic follow the general pattern of observation. The velocity ground motion is a clear long period pulse that exhibit in the three components.

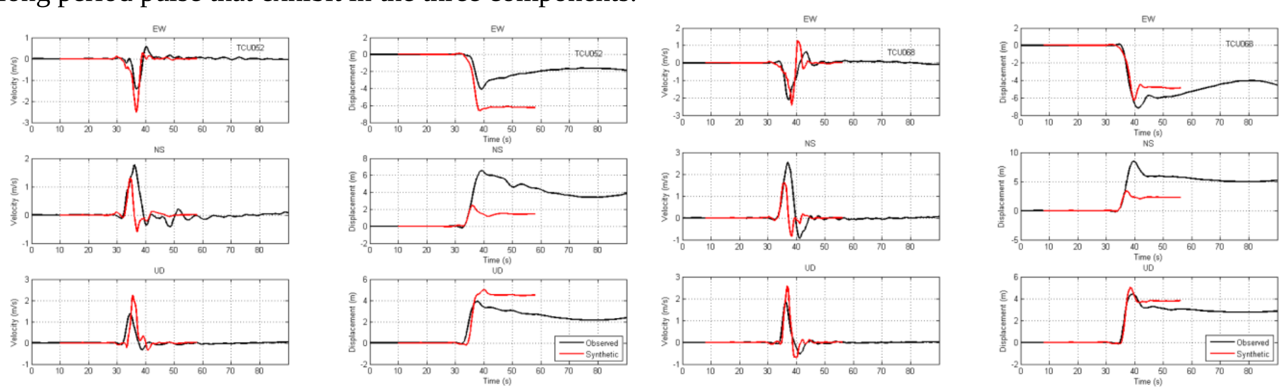

Fig. 6 Comparison with observed data of displacement and velocity ground motion at some selected station that with permanent displacement

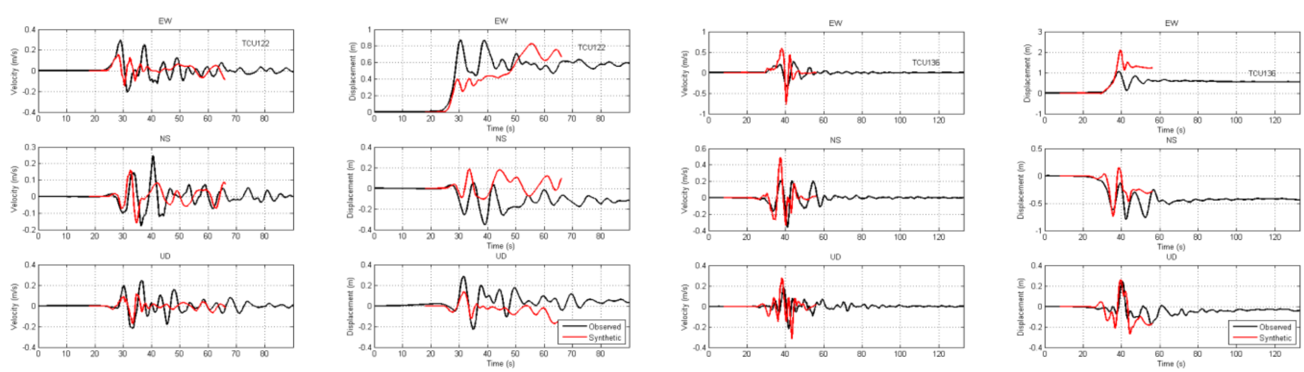

Fig. 6 (continuation) Comparison with observed data of displacement and velocity ground motion at some selected station that with permanent displacement

5.3 Effects of zero stress drop at the shallow zone

We evaluate the effect of zero stress drop at the shallow zone. The asperity and background are the same as the preferred model. Zero stress drop implies that the frictional strength drops to the level of the initial stress, that is contrary to our preferred model in which frictional strength behave with strength hardening during rupture.

Fig. 7 shows a comparison of the slip and peak slip velocity between these two models. Though peak slip velocity is similar at the seismogenic zone, the model with zero stress drop predicts the largest values at the free-surface of the northern site. The slip distribution of the model with zero stress drop is higher over all the fault than the model with negative stress drop. The largest values are predicted at the free-surface and the moment magnitude is Mw=7.7. It suggests that zero stress drop significantly enhance the size of the earthquake. Permanent displacement also increases to very high values as shown in Figure 8. These figure shows the permanent horizontal displacement for the two models. Both models show the rotation at the northern part of the horizontal displacement, as earlier mentioned. As described before, this rotation of the ground motion is due to the rupture directivity along the strike of dipping faults that break the free-surface. The rotation increases with the propagation distance due to the interaction of the rupture propagation with the free-surface. As a consequence, the amplitude of fault parallel component significantly increases to values comparable to the fault normal component

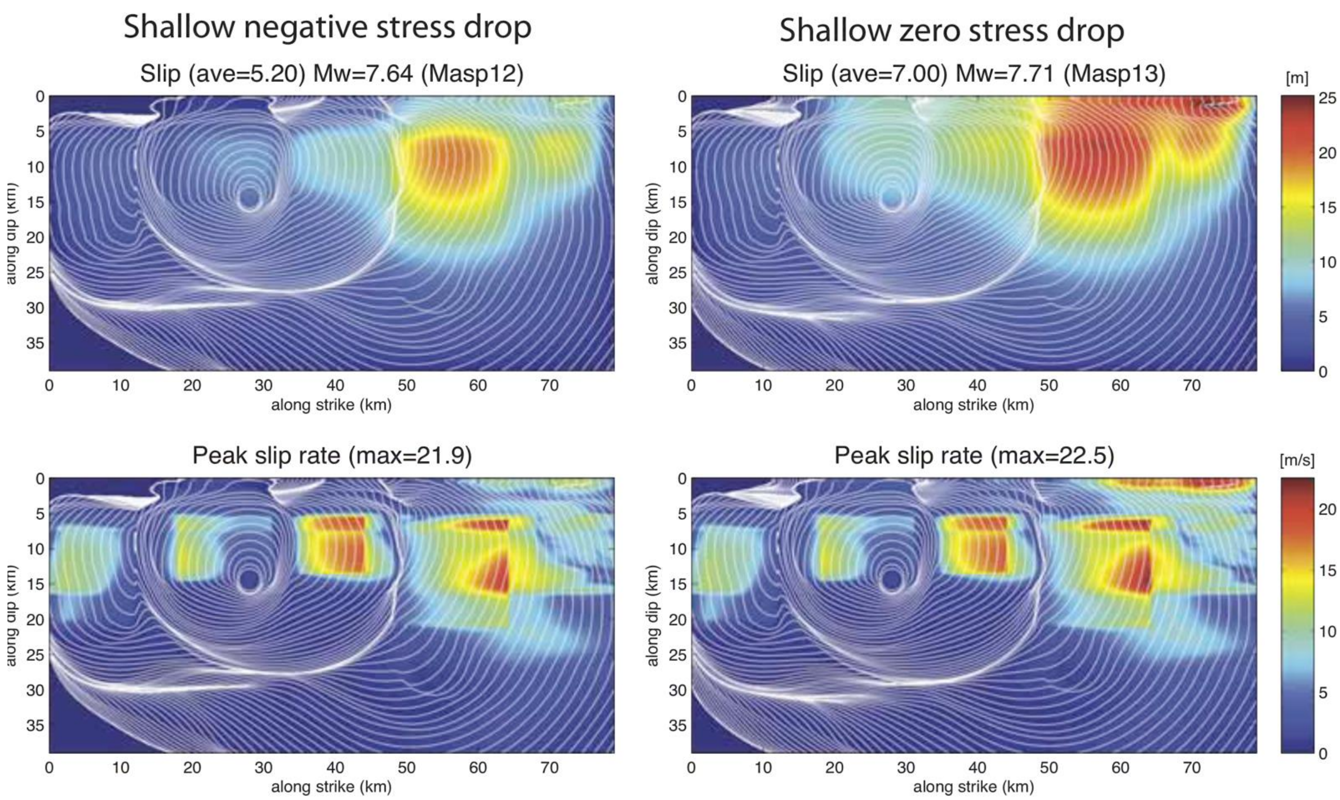

Fig.7 Dynamic rupture solution represented by the final slip distribution (top) and peak slip velocity (bottom) for the asperity models with negative stress drop at the shallow zone (left) and with zero stress drop at the shallow zone (right). Contour lines on the slip and peak slip rate images are the rupture time each 0.5 seconds.

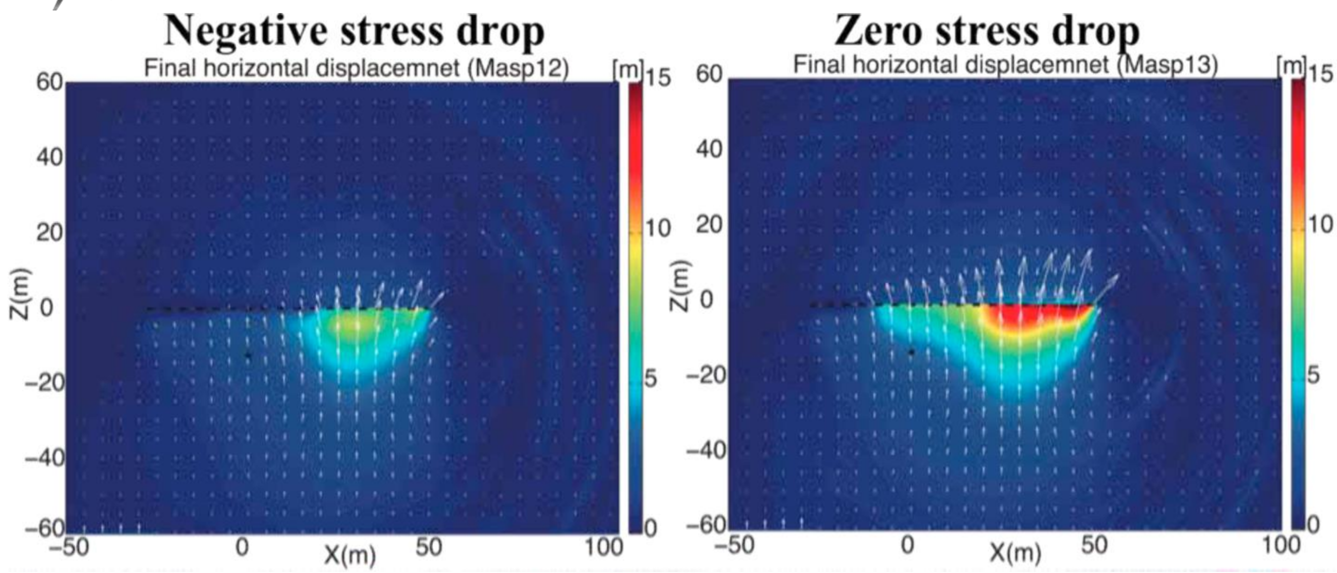

Fig. 8 Final horizontal displacement for the asperity models with negative stress drop at the shallow zone (left) and with zero stress drop at the shallow zone (right). Arrows represent the direction of the displacement vector. Dashed black line is the trace of the fault intersecting the free-surface. Black star is the epicenter. Right side is the northern

5.3 Effects of buried rupture depth

Here we want to evaluate the effect depth of a buried rupture. For this purpose we forced our rupture model to suddenly stop at 1.0km and 2.0km from the free-surface, i.e., no surface rupturing. To do it we assumed that the frictional strength in this zone is infinite. Figure 9 shows the slip distribution for these two models. The model with 1km buried depth successfully propagates over almost all the allowed rupture area, breaking all the asperities. However, the rupture model with 2km depth stops after braking the first two asperities, resulting in a small event of Maginitute Mw=6.9. This suggests that when the shallow zone breaks, rupture further extends along strike.

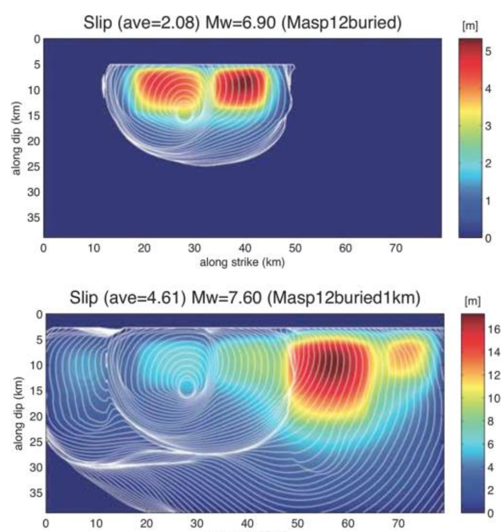

Fig. 9 Final slip distribution from asperity models with fault buried 2km depth (top) and buried 1km depth (bottom). Contour lines on the slip images are the rupture time each 0.5 seconds.

6. Conclusions

We use spontaneous dynamic rupture models to investigate the shallow zone effects on surface rupturing earthquakes of reverse faults and the corresponding permanent displacement. The 1999 Chi-Chi, Taiwan earthquake is used as a case study. The problem is tackled using asperity models. The asperities parameterization for dynamic rupture simulations has its basis on the asperity model characterization of Dalguer et al [11, 20], Somerville et al [16] and Kamae and Irikura [23]. As a case study we use the 1990 Mw 7.6 Chi-Chi, Taiwan, Earthquake. The main conclusions of our investigation for a reverse fault rupture are as follow:

-The asperities are the main driver elements to break the shallow layer and free-surface

-The shallow layer with zero stress drop produces larger slip and peak slip velocities than the one with negative stress drop. Zero stress drop on the shallow zone may over-predict ground motion and permanent displacement, leading to unrealistic scenarios.

-The rupture propagation directivity along the strike for reverse faults that break the freesurface produces horizontal rotation of the ground motion and permanent displacement. This phenomenon results in an increasing of the fault parallel component, reaching to significant values comparable to the fault normal component at long propagation distance of the rupture.

-Buried rupture inhibits the extension of the fault rupture along strike, and consequently the permanent fault displacement. In our case study, if rupture stop at 2.0km depth (i.e. it does not break the shallow layer) the rupture along strike stops earlier. However, at 1km depth, the rupture successfully extends along the whole fault area. This suggests that when rupture approaches to the free surface, the chance to the rupture become larger along strike significantly increases.

-With this study we show that the shallow layer representation in the earthquake modeling play an important role on fault displacement and near source ground motion generation.

7. References

[1] Abrahamson NA (2002): Velocity pulses in near-fault ground motions, *in Proceedings of the UC Berkeley—CUREE Symposium in Honor of Ray Clough and Joseph Penzien*: Berkeley, California, UC Berkeley, Consortium of Universities for Research in Earthquake Engineering, 9–11 May 2002, 40–41.

[2] Burks LS, Baker JW (2014): Fling in near-fault ground motions and its effect on structural collapse capacity, *in Tenth U.S. National Conference on Earthquake Engineering, Frontiers of Earthquake Engineering*, Anchorage, Alaska, 21–25 July 2014.

[3] Kamai R, Abrahamson N, Graves R (2014) : Adding Fling Effects to Processed Ground-Motion Time Histories. *Bull. Seism. Soc. Am.*, Vol. 104, No. 4, pp. 1914–1929, August 2014, doi: 10.1785/0120130272.

[4] Akkar S, Gülkan P (2002): A Critical Examination of Near-Field Accelerograms from the Sea of Marmara Region Earthquakes, *Bull. Seism. Soc. Am.* **92**, 1, pp. 428–447.

[5] Shin TC, Teng TL (2001): An overview of the 1999 Chi-Chi, Taiwan, earthquake, *Bull. Seism. Soc. Am.* **91,** 895–913.

[6] Dalguer LA, Irikura K, Riera J, Chiu HC (2001) : The Importance of the Dynamic Source Effects on Strong Ground Motion During the 1999 Chi-Chi (Taiwan) Earthquake: Brief Interpretation of the Damage Distribution on Buildings. *Bull. Seismol. Soc. Am*., 95, 1112-1127.

[7] Dreger D, Hurtado G, Chopra A, Larsen S (2011): Near-Field Across-Fault Seismic Ground Motions, *Bull. Seism. Soc. Am.*, Vol. 101, No. 1, pp. 202–221, February 2011, doi: 10.1785/0120090271

[8] Lu M, Jun Li X, Wen An X, Zhao J.X (2010): A Preliminary Study on the Near-Source Strong-Motion Characteristics of the Great 2008 Wenchuan Earthquake in China, *Bull. Seism. Soc. Am.*, Vol. 100, No. 5B, pp. 2491–2507, November 2010, doi: 10.1785/0120090132.

[9] Galvez P, Dalguer LA, Ampuero JP, Giardini D (2016): Rupture reactivation during the 2011 Mw 9.0 Tohoku earthquake: Dynamic rupture and ground motion simulations, *Bull. Seismol. Soc. Am.*, Vol. 106, No. 3, pp. –, June 2016, doi: 10.1785/0120150153.

[10] Somerville PG, Smith NF, Graves RW, Abrahamson NA (1997): Modification of empirical strong ground motion attenuation relations to include the amplitude and duration effects of rupture directivity, *Seism. Res. Lett.* **68,** 199–222.

[11] Dalguer LA, Miyake H, Day SM, Irikura K (2008): Surface Rupturing and Buried Dynamic Rupture Models Calibrated with Statistical Observations of Past Earthquakes. *Bull. Seismol. Soc. Am.* 98, 1147-1161, doi: 10.1785/0120070134.

[12] Pitarka A, Dalguer LA, Day SM, Somerville P, Dan K (2009): Numerical study of ground motion differences between buried and surface-rupturing earthquakes, *Bull. Seism. Soc. Am.*, Vol. 99, No. 3, pp. 1521–1537, June 2009, doi: 10.1785/0120080193.

[13] Miyake H, Iwata T, Irikura K (2003): Source characterization for broadband ground-motion simulation: kinematic heterogeneous source model and strong motion generation area, *Bull. Seismol. Soc. Am*. 93, 2531–2545.

[14] Irikura K, Miyake H (2011): Recipe for predicting strong ground motion from crustal earthquake scenarios, Pure Appl. Geophys., 168, 85-104, doi:10.1007/s00024-010-0150-9.

[15] Wells DL, Coppersmith KL (1994): New empirical relationships among magnitude, rupture width, rupture area, and surface displacement, Bull. Seismol. Soc. Am. 84, 974–1002.

[16] Somerville P, Irikura K, Graves R, Sawada S, Wald D, Abrahamson N, Iwasaki Y, Kagawa T, Smith N, Kowada A (1999): Characterizing crustal earthquake slip models for the prediction of strong ground motion, *Seism. Res. Lett.* 70, 59–80.

[17] Hanks TC, Bakun WH (2002): A bilinear source-scaling model for M-log A observations of continental earthquakes, *Bull. Seismol. Soc. Am.* 92, 1841–1846.

[18] Miyakoshi K (2002): Source characterization for heterogeneous source model, *Chikyu Mon. Extra* 37, 42–47 (in Japanese).

[19] Murotani S, Matsushima S, Azuma T, Irikura K, Kitagawa S (2015): Scaling Relations of Source Parameters of Earthquakes Occurring on Inland Crustal Mega-Fault Systems, *Pure Appl. Geophys.* 172, 1371–1381; DOI 10.1007/s00024-014-1010-9.

[20] Dalguer LA, Miyake H, Irikura K (2004) : Characterization of dynamic asperity source models for simulating strong ground motion, *Proceedings of the 13th World Conference on Earthquake Engineering (13WCEE)*, Vancouver, B.C., Canada, August 1-6, 2004, Paper No. 3286.

[21] Dalguer LA, Irikura K, Zhang W, Riera JD (2002):Distribution of Dynamic and Static Stress Changes during 2000 Tottori (Japan) Earthquake: Brief Interpretation of the Earthquake Sequences; Foreshocks, Mainshock and Aftershocks, *Geophys. Res.Lett.*, 29(16), 1758, doi:10.1029/2001GL014333.

[22] Zhang W, Iwata T, Irikura K, Sekiguchi H, Bouchon (2003): Heterogeneous distribution of the dynamic source parameters of the 1999 Chi-Chi, Taiwan, earthquake, *J. Geophys. Res.*, 108, NO. B5, 2232, doi:10.1029/2002JB001889.

[23] Kamae K, Irikura K (1998): Source model of the 1995 Hyogo-ken Nanbu earthquake and simulation of near-source ground motion, *Bull. Seismol. Soc. Am.*, 88, 2, 400-412.

[24] Marone C (1998): Laboratory-derived friction laws and their application to seismic faulting, *Ann. Revs. Earth Plan. Sci.* 26, 643–696.

[25] Marone C, Scholz CH (1988): The depth of seismic faulting and the upper transition from stable to unstable slip regimes, *Geophys. Res. Lett.* 15, 621–624.

[26] Dalguer LA, Irikura K, Riera J (2003) : Generation of New Cracks Accompanied by the Dynamic Shear Rupture Propagation of the 2000 Tottori (Japan) Earthquake, *Bull. Seismol. Soc. Am.*, 93, 2236-2252.

[27] Dalguer LA, Irikura K, Riera J (2003) : Simulation of Tensile Crack Generation by 3D Dynamic Shear Rupture Propagation During an Earthquake. *J. Geophys. Res.*,108(B3), 2144, doi:10.1029/2001JB001738.

[28] Shi Z, Day SM (2013): Rupture dynamics and ground motion from 3-D rough-fault simulations *J. Geophys. Res.* , 118, doi:10.1002/jgrb.50094.

[29] Roten D, Olsen KB, Day SM, Cui Y, Fah D (2014): Expected seismic shaking in Los Angeles reduced by San Andreas Fault zone plasticity , *Geophys. Res. Lett.* , 41, doi:10.1002/2014GL059411

[30] Ben-Zion Y, Peng Z, Lewis MA, McGuire J (2007): High Resolution Imaging of Fault Zone Structures With Seismic Fault Zone Waves, *Scientific Drilling*, Special Issue No. 1, 78-79, doi:10.2204/iodp.sd.s01.23.2007, 2007.

[31] Vermilye JM, Scholz CH (1998): The process zone: a microstructural view of fault growth, *J. Geophys. Res.* 103, 12,223–12,237.

[32] Brune JN, Anooshehpoor A (1998): A physical model of the effect of a shallow weak layer on strong ground motion for strike-slip ruptures, *Bull. Seismol. Soc. Am.* 88, 1070–1078.

[33] Day SM, Ely GP (2002): Effect of a shallow weak zone on fault rupture: Numerical simulation of scale-model experiments, *Bull. Seismol. Soc. Am.* 92, 3006–3021.

[34] Shin TC, Kuo KW, Lee WHK, Teng TL, Tsai YB (2000): A preliminary report on the 1999 Chi-Chi (Taiwan) Earthquake, *Seism. Res. Lett*. 71, 24–30.

[35] Iwata T, Sekiguchi H, Irikura K (2000): Rupture process of the 1999 Chi-Chi, Taiwan, earthquake and its near-source strong ground motions, *Proc. International Workshop on Annual Commemoration of Chi-Chi earthquake*, Taipei, Taiwan, Vol.1, 36-46, Sep.

[36] Zhang W, Iwata T, Irikura K, Sekiguchi H, Bouchon M (2003): Heterogeneous distribution of the dynamic source parameters of the 1999 Chi-Chi, Taiwan, earthquake, *J. Geophys. Res.*, 108, NO. B5, 2232, doi:10.1029/2002JB001889.

[37] Ikeda T, Kamae K, Miwa S, Irikura K (2004): Source modeling and strong ground motion simulation for the 1999 Chi-Chi, Taiwan earthquake, *Proceedings of the 13th World Conference on Earthquake Engineering (13WCEE)*, Vancouver, B.C., Canada, August 1-6, 2004, Paper No. 1289.

[38] Andrews DJ (1976): Rupture velocity of plane-strain shear cracks, *J. Geophys. Res.*, 81, 5679-5687.

[39] Ely G, Day SM, Minster JB (2009): A support-operator method for 3D rupture dynamics, *Geophysical Journal International*, 177 1140-1150, DOI: 10.1111/j.1365246X.2009.04117.x.

[40] Dalguer LA, Irikura K, Riera J, Chiu HC (2001): The Importance of the Dynamic Source Effects on Strong Ground Motion During the 1999 Chi-Chi (Taiwan) Earthquake: Brief Interpretation of the Damage Distribution on Buildings. *Bull. Seismol. Soc. Am.*, 95, 1112-1127.

[41] Azuma T, Sugiyama Y, Kariya Y, Awata Y, Lee YH, Shih TS, Lu ST, Wu WY (2000): Displacements and segmentation of the surface fault associated with 1999 Chi-Chi, Taiwan, earthquake, *Annual Report on Active Fault and Paleoearthquake Researches*, no.EQ/00/2, pp. 221-235.

[42] Lee WHK, Shin TC, Kuo KW, Chen KC Wu CF (2001): CWB Free-Field Strong-Motion Data from the 21 September Chi-Chi, Taiwan, Earthquake. *Bull. Seismol. Soc. Am.*, 91(5), pp. 1370–1376,